International Conference on Space Optics—ICSO 2018

Chania, Greece

9–12 October 2018

Liquid crystal phase modulator integration on the TriPleX photonic platform

K. Wörhoff

A. Ryabchun

M. Hoekman

J. Epping

et al.

Liquid crystal phase modulator integration on the TriPleX photonic platform

K. Wörhoff[1], A. Ryabchun[2], M. Hoekman[1], J. Epping[1], R. Grootjans[1], and A. Leinse[1]

[1] LioniX International, PO Box 456, 7500 AL Enschede, The Netherlands

[2] University of Twente, MESA+ Institute for Nanotechnology, PO Box 217, 7500 AE Enschede, The Netherlands

ABSTRACT

Technology integration of liquid crystal cells for electro-optic modulation has been implemented on the commercial TriPleX photonic platform. Design and fabrication procedure have been optimized for fulfilling the low insertion loss criterion for applications such as space communication and enabling the implementation of compact liquid crystal tuning elements for achieving high integration density. First performance testing of this concept has confirmed low-power consumption switching with 2π phase tuning being obtained within a voltage range of 2.5 V.

Keywords: liquid crystal, photonic platform, TriPleX, phase modulator, on-chip integration

1. INTRODUCTION

The versatile TriPleX photonic platform [1] of *LioniX International* is based on alternating dielectric Si_3N_4 and SiO_2 layers, fabricated with CMOS compatible equipment. TriPleX waveguide channels perform at low loss over a wide wavelength range (400 nm-2.35 μm). Moreover, low-loss vertical spotsize convertors can be implemented in this technology to enable efficient on-chip integration of low and high contrast waveguide sections. This allows simultaneously for high on-chip integration density, optimized interfaces to fiber connections as well as hybrid chip-to-chip assemblies with active platforms such as InP [2].

As concluded in a recent ESA desk study (Application of Satellite On-board Optical Beam Forming AO/1-6955/11/NL/NR), the TriPleX waveguide technology is highly suited for Optical Beam Forming Network (OBFN) applications [3][4]. However, the currently required power levels for thermo-optic tuning (approximately 0.5 W per tuning element) prohibit the implementation of complex devices with a high channel count. Therefore, the strong need for low-power (electro-optic) phase tuning is evident. A highly promising route towards significant tuning power reduction is addressed by integrating Liquid Crystal (LC) cells in the back-end process of the TriPleX chip fabrication. Goal of the development presented in this paper is the demonstration of LC-based phase tuning on the TriPleX platform by locally replacing part of the waveguide oxide top cladding by a suited Liquid Crystal material. Furthermore, the development of a concept for usage of this technology in commercial space applications will be envisaged.

This paper starts with the LC cell integration principle and waveguide design taking the application boundaries into account. Then the fabrication of the demonstrator device will be addressed. Finally, test results are discussed.

2. INTEGRATION DESIGN

2.1 Integration principle and design boundaries

The liquid crystal modulator will be locally implemented in the cladding section of the TriPleX waveguide channel as can be seen from the schematic drawing in Figure 1 (left). To avoid excessive leakage of light in the modulator section, the effective refractive index (N_{eff}) of the waveguide channel has to be larger than the refractive index of the liquid crystal material throughout the applied tuning range. For overall propagation loss minimization, the interface loss (chip –

modulator interface) has to be considered as well. Low modal overlap mismatch between both section will favor minimized loss figures.

From the OBFN application and space compatibility point of view the following requirements can be defined for the design: (1) operation wavelength: 1550 nm, (2) light polarization: TE, (3) length of modulator section: ≤ 1 mm, (4) insertion loss per modulator: < 0.01 dB, (5) 2π tuning voltage: < 5 V, (6) modulation speed: < 1 ms, and (7) resistance to harsh environments (temperature, radiation). Based on these boundaries a basic waveguide geometry with an electrode configuration as schematically depicted in Figure 1 (right) will be applied for the design calculations. A liquid crystal cell of width w and thickness d will be implemented above the waveguide channel. The horizontal electrode configuration enables switching of TE-polarized light propagating through the waveguide channel given the liquid crystal molecules are aligned with their high refractive index axis (n_e) in the propagation direction.

The chosen TriPleX waveguide configuration is an asymmetric double stripe (ADS) geometry. This specific geometry, shown in Figure 2, allows for combining low contrast channel waveguides enabling low-loss fiber connection with high contrast channel waveguides suited for compact functional designs required by the OBFN application [1]. Moreover, the high contrast section fulfills the high N_{eff} requirement for LC material integrated in the waveguide cladding.
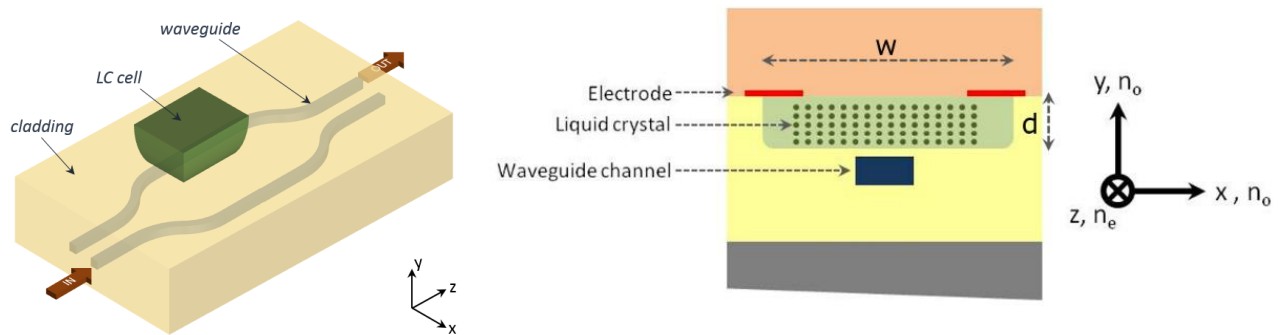

Figure 1. Schematic view of an arbitrary optical waveguide with LC cell integrated in the top cladding (left). Cross-section of principal waveguide geometry and electrode configuration for the LC modulator integration on TriPleX with n_e and n_o being the extraordinary (high) and ordinary (low) refractive index axis, respectively (right). (dimensions not to scale)
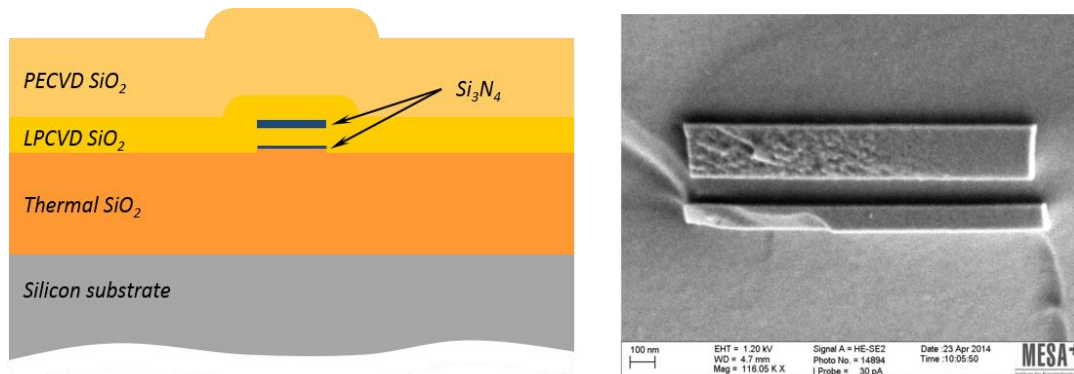

Figure 2. Schematic layout of TriPleX waveguide cross-section with asymmetric double stripe geometry (left), SEM image of fabricated ADS waveguide (right). [1]

2.2 Design of integrated LC cell

There is a wide range of liquid crystal materials with different characteristics [5]. For compact integrated switches and modulators nematic LC material with a reasonably large birefringence $\Delta n > 0.1$ ($\Delta n = n_e - n_o$) is required. Moreover, the nematic temperature range of the material should cover a wide range for being compliant with the environmental

requirements of space applications. Such LC properties can be fulfilled by eutectic mixtures of several nematic liquid crystal materials. Some selected examples of the nematic temperature ranges of different LCs are given in Table 1.

Table 1. Properties of wide nematic range LC materials: melting temperature T_M and clearing point T_C [6][7].

LC type	E7	ZLI-4792	E100	E43	ROTN200	NP1291TNC	NP1694
T_M [^{0}C]	-10	-40	-20	-10	-20	-10	-20
T_C [^{0}C]	60.5	92	78	84	65.2	107	86

A suited eutectic LC mixture was chosen and the optical properties were implemented in the numerical design tools. The TriPleX – LC waveguide design in terms of layer thicknesses and channel widths has been optimized by applying PhoeniX design software [8]. The expected device performance has been calculated for the optimized TriPleX ADS geometry. Dependent on the exact device geometry and the LC director angle (θ), modulator lengths ($L_{2\pi}$) ranging from 3 mm down to 100 µm have been calculated for obtaining a 2π phase shift.

Since a large number of modulators has to be implemented in the OBFN devices, the optical loss induced in the modulator should be minimized. Two loss contributions have been calculated: the propagation loss in the LC cell section and the transition loss at the interface of the LC cell. For the propagation loss, an effective loss calculation based on modulation in a Mach-Zehnder interferometer (MZI) configuration has been made. In this calculation the nematic director in one MZI branch is kept at 0 degrees, whereas the angle θ in the other branch is tuned. Taking the required modulator length $L_{2\pi}$ into account, the effective propagation loss (α_{eff}) can be calculated by ($\frac{1}{2}$ $L_{2\pi}$ [$\alpha(\theta)+\alpha(0)$]). The calculated effective propagation is shown in Figure 3 (left) and can be kept below 5 x 10^{-3} dB per modulator. For abrupt cell window interfaces, the transition losses as a function of waveguide width are shown in Figure 3 (right) for different LC tuning angles θ ranging from 0 to 30^0. For LC tuning angles up to 15^0 the transition loss criterion of 0.01 dB can be fulfilled. For larger tuning angles tapering of the LC cell window transition will be required.
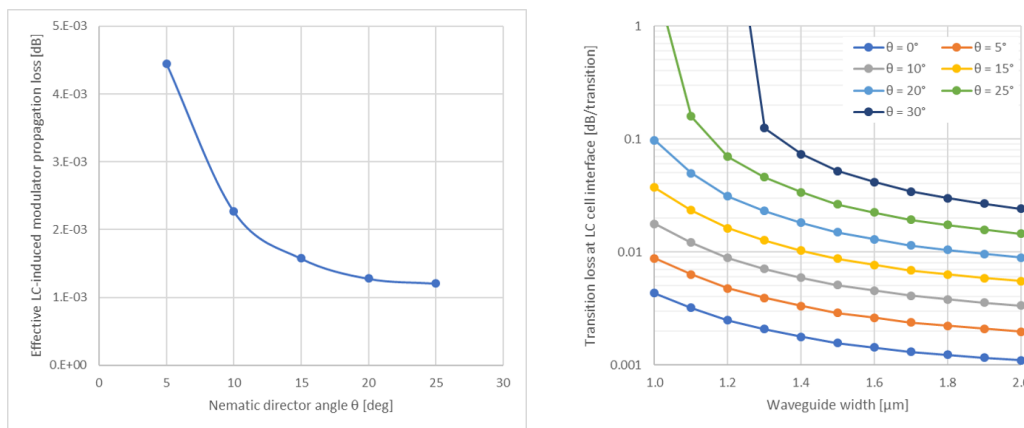

Figure 3. Effective LC-induced modulator propagation loss as a function of θ, where the angle between waveguide propagation direction and nematic director is 0° in one MZI branch and θ in the other branch (left). Transition loss for an abrupt transition from LC waveguide to fully SiO_2 cladded waveguide as a function of waveguide width and angle θ as parameter (right).

The simulation results have been implemented in a mask set for the TriPleX – LC cell chip fabrication. The main test feature is a set of MZI-based tuning elements with LC cell and electrode configuration as depicted in the mask screenshot of Figure 4. The modulator sections (electrode lengths) have been varied in length ranging from 30 µm to 5 mm.
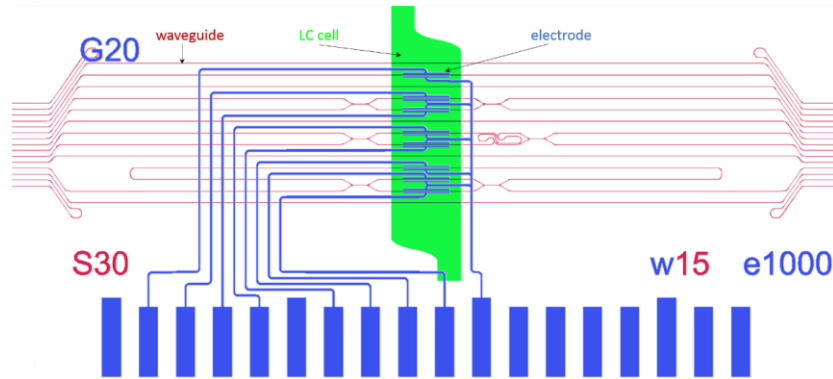
Figure 4. Mask layout of modulator test chip with set of MZI-based waveguide structures (red), LC cell window (green) and electrode configuration (blue). The electrode length of this specific chip is 1 mm.

3. DEVICE FABRICATION

3.1 Fabrication flow

In the fabrication flow we distinguish three fabrication parts of which the main steps are as follows:

(1) Fabrication of the waveguide chips with LC cell windows:
In this step the TriPleX waveguides are fabrication on a silicon substrate. The wafer-scale processing is based on LioniX' standard platform technology. The LC cell windows are implemented through lithography and etching into the top cladding of waveguide wafer. Finally, the chips are diced.

(2) Fabrication of the cover plate wafer with electrodes:
The electrode pattern is fabricated by lithography and metal deposition onto a transparent fused silica wafer. Then the cover plates are diced.

(3) Assembly of waveguide and cover parts on chip level:
Waveguide chips and cover plates are coated with a photoalignment layer. This enables the LC alignment in the cell by a contactless method, photoalignment [9][10]. Then chip and electrode plate are aligned and fixed by glue. In the final step, the cell filling is performed including UV illumination, LC filling process, and cell sealing.

A schematic of the assembled TriPleX – LC chip is depicted in the cross-sectional view of Figure 5.
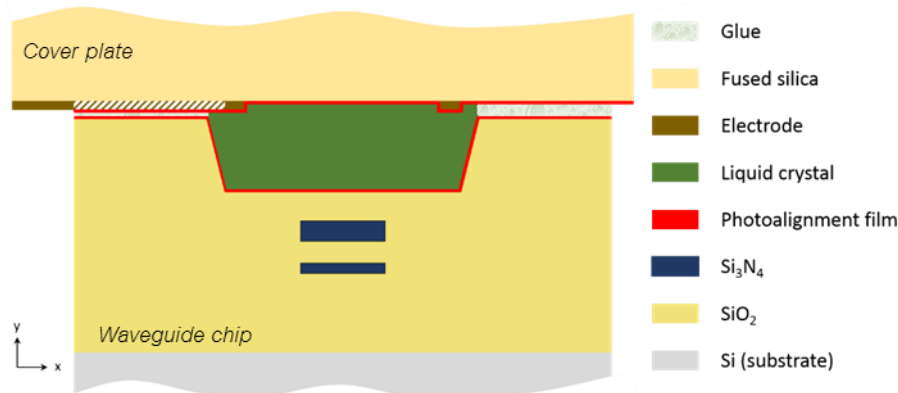

Figure 5: Schematic cross-section of TriPleX – LC cell assembly (dimensions not to scale).

3.2 Chips fabrication and inspection

TriPleX waveguide chips with integrated LC cell windows as well as the electrode cover plates have been fabricated in line with the above described procedure. Prior to assembly and cell filling, the quality of the chips has been inspected. The optical quality is assessed by light propagation applying red light coupling. A photograph of light propagating through a waveguide chips with LC windows is shown in Figure 6. It can be seen that light propagation is excellent and no significant loss has been observed either in the window or at the window – SiO$_2$ cladding transition. Then the full assembly procedure has been carried out. The quality of the liquid crystal cell filling step was assessed by microscope inspection. Polarized optical microscopy has been applied to confirm the correct alignment of the liquid crystal material in the cells (Figure 7). Uniform planar alignment and defect-free cell filling is evident.
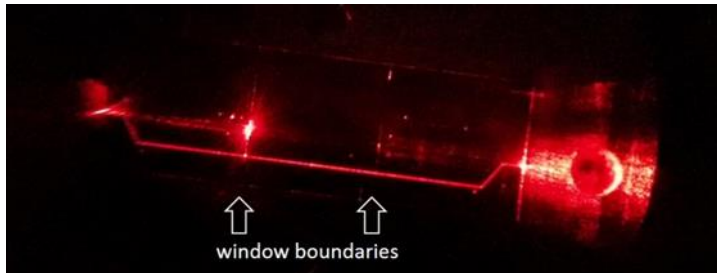

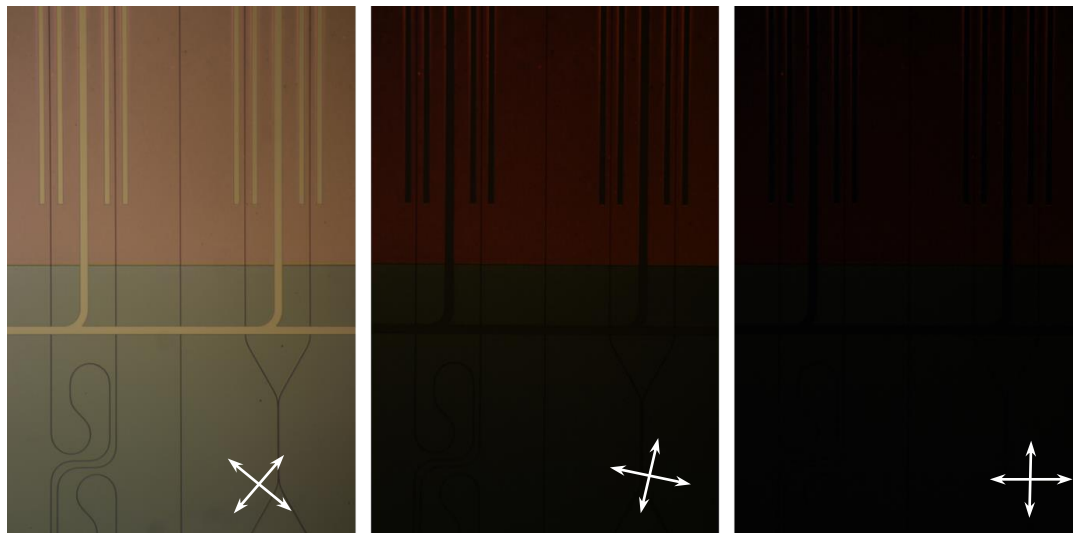Figure 6: Red light propagation through chip before photoalignment coating and assembly.

Figure 7: Polarized optical microscope images of assembled chip after LC cell filling for different polarization states. LC alignment is vertical (in plane of the picture) and cross polarizer settings are indicated by the white arrows.

4. SWITCHING RESULTS

4.1 Measurement procedure

The principle of the switching device is based on LC tuning of an MZI waveguide section. The MZI layout in the waveguide layer along with the LC cell area and the relevant electrode configuration is shown in Figure 8. Light is entering into one branch of the device from the left side. After the first splitter the light will be distributed over both MZI branches. Thereafter it enters the area of the LC cell. After passing the LC area (without applied voltage) the light is combined by the second splitter into the output port 2. In case a voltage is applied to one of the electrodes, the liquid crystal in-between the powered electrode set is changing its orientation. Consequently, the effective refractive index and

the light path change for the channel in-between these electrodes. Due to the phase difference of the light from both branches at the second splitter, the light intensity at both output ports will be tuned. In the characterization this will be monitored as a voltage-dependent fringe pattern on one of the output ports.

For driving the switching device on the measurement stage, a submount is needed to connect the electrical ports on the chip to the electronics. A picture of the fabricated submount with a test chip is shown in Figure 9 (left). The electrodes on the chip are connected to the electrodes on the PCB unit as can be seen from the detail in Figure 9 (right). On the PCB unit a flatcable connection to the driver unit is integrated. The chip and the PCB unit are fixed on a copper mount which fits onto the measurement stage.
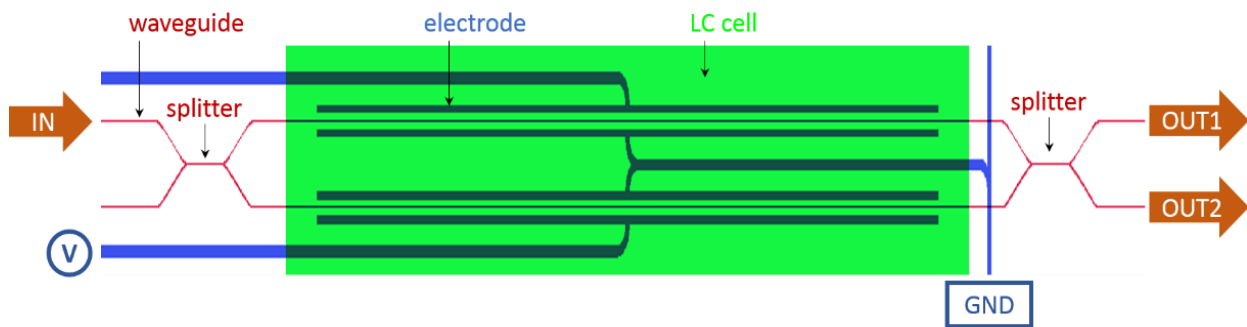

Figure 8: Detail of functional chip layout with simple MZI configuration.

For LC switching the inherent properties of the LC response are of importance [11]. The typical nematic LC molecule aligns to the applied field through an induced dipole interaction. This means, the molecules respond to the magnitude of the field regardless the sign. Another effect that occurs in LC material is ion-migration inducing response effects on various time scales. On short timescale ion-migration is causing shielding, which result in cancelling the applied voltage and relaxation of the LC molecule. On longer timescale ion-migration leads to permanent charging causing burn-in and permanent material degradation. Therefore, switching of the photonic device has to be driven by an AC voltage with minimized DC offset. The AC voltage initiates the (sign-independent) dipole response, whereas the minimized DC offset serves the DC-balance constraint. The ideal waveform that satisfies these requirements is a square wave with zero DC offset. Rapid switching of the voltage polarity basically provides a constant field magnitude to the LC material while ion-migration is suppressed. These demands were taken into account upon selection of an appropriate driver unit.
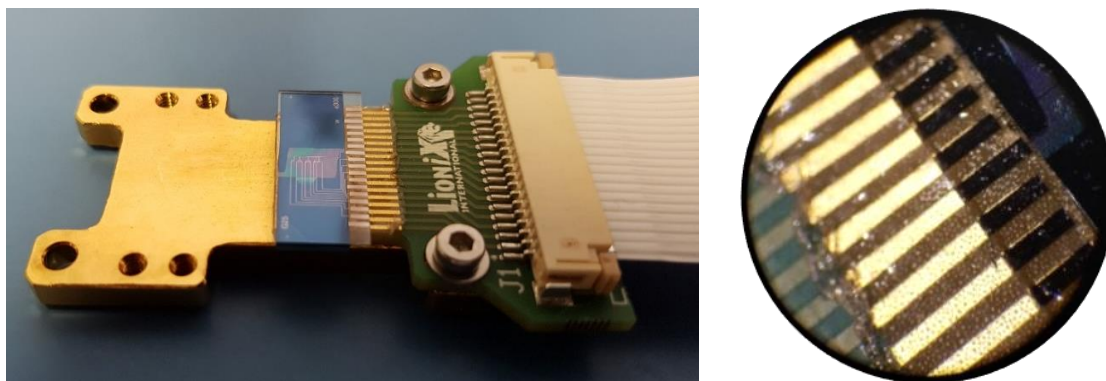

Figure 9: Picture of submount with LC switching chip (left) and detail of electrode connection (right).

4.2 Measurement results

The assembled chips were mounted to the measurement stage and tested for light propagation and switching behavior. Snapshots of a switching video of a chip with 3 mm electrode length are shown in Figure 10. It can be clearly seen how the light distribution over the two output channels of the MZI (left hand side of pictures) changes.

Following this initial proof of LC-based switching more detailed measurements have been carried out. MZI signal tuning was captured on the oscilloscope along with the corresponding driver voltage output (manual ramping). As it can be seen in Figure 11, the device is tuning over six 2π fringes within a voltage range of about 15 V (taking linear part of response curve into account). Consequently, 2π phase tuning can be achieved with 2.5 V tuning range.
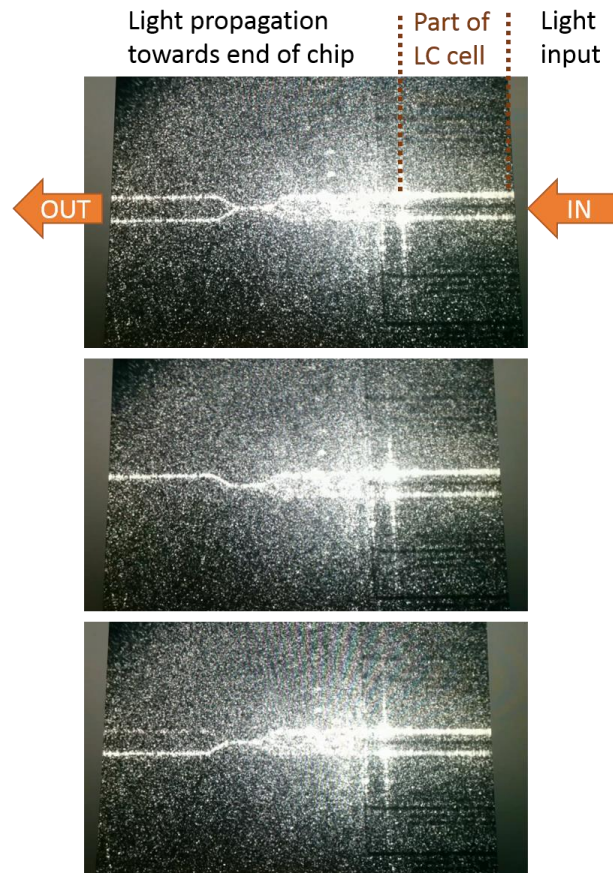

Figure 10: Snapshots of light switching by LC tuning of fully assembled chip with equal light distribution over both output channels (top), switching to the upper output port (center) and to the lower output channel (bottom).
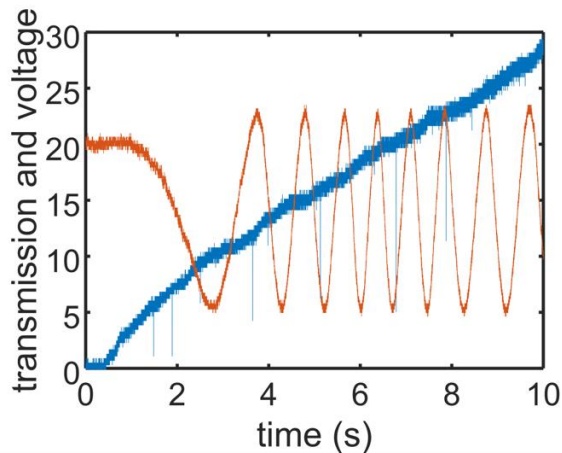

Figure 11: Modulator response (red) and applied voltage from driver unit (blue) for LC- TriPleX test chip.

In order to assess the power consumption of the LC-based devices vs. switching with classical heater elements, the current under operation over the driver voltage range has been monitored. For the full assembly about 30 µW power dissipation was calculated upon a driver voltage of 30V. Finally, a few preliminary measurements on the LC switching dynamics have been carried out. The LC response on voltage ramp speed varying from 0.01 Hz to 0.5 Hz has been monitored and the LC relaxation behavior has been measured. Interpretation of these results and optimization of the switching response will be subject to upcoming R&D tasks.

5. SUMMARY AND CONCLUSION

In this ESA-funded R&D activity liquid crystal cells for signal switching and modulation have been integrated into the cladding material of the TriPleX photonic platform. A concept for operation at 1550 nm wavelength with TE polarized light has been developed taking boundary conditions such as low insertion loss (< 0.01 dB/modulator), feasibility for short modulator length (< 1 mm) and low 2π tuning voltage (< 5V) into account. The demonstrator device has been designed accordingly. Chip fabrication has been carried out and the assembly process for the TriPleX – LC cell realization has been developed. Light coupling to the demonstrator units has confirmed good propagation properties throughout the LC cell. Light switching has been demonstrated in Mach-Zehnder interferometer structures. In the linear response regime of the LC switches 2π phase tuning can be realized within a voltage range of 2.5 V. First dissipation measurements have shown a reduction in power consumption of about four orders of magnitude as compared to switches actuated by heater elements. Further understanding of LC dynamics and optimization of the switching procedure has to be addressed in follow-up research.

It can be concluded that demonstrating phase tuning in an integrated optical waveguide with low electrical power has been achieved while the low loss properties of the waveguide was maintained. The proof of concept has been implemented into a waveguide geometry of LioniX' photonic technology platform enabling amongst others Optical Beam Forming Network applications for space. Next development steps will focus on aspects such as further device optimization including integration with functional application designs (e.g. OBFNs), wafer scale assembly procedures and fabrication scaling for commercialization of LC-based modulation and switching.

ACKNOWLEDGEMENTS

REFERENCES

[1] Wörhoff, K., Heideman, R.G., Leinse, A., and Hoekman, M., "TriPleX: a versatile dielectric photonic platform," Adv. Opt. Techn. 4(2), 189–207 (2015).

[2] Roeloffzen, C.G.H., Hoekman, M., Klein, E.J., Wevers, L.S., Timens, R.B., Marchenko, A., Geskus, D., Dekker, R., Alippi, A., Grootjans, R., van Rees, A., Oldenbeuving, R., Epping, J.P., Heideman, R.G., Wörhoff, K., Leinse, A., Geuzebroek, D.H., Schreuder, E., van Dijk, P.W.L., Visscher, I., Taddei, C. Fan, Y., Taballione, C., Liu, Y., Marpaung, D.I.A., Xhuang, L., Benelajla, M., and Boller, K. J., "Low loss Si3N4 TriPleX optical wavegudies: Technology and applications overview," IEEE J Sel. Top. Quant. Electr. 24 (4), 4400321 (2018).

[3] Roeloffzen, C.G.H., Oldenbeuving, R.M., Timens, R.B., van Dijk, P.W.L., Taddei, C., Leinse, A., Hoekman, M., Heideman, R.G., Zhuang, L., Marpaung, D.A.I., and Burla, M., "Integrated optical beamformers," Proc. OFC, Tu3F.4 (2015).

[4] Anzalchi, J., Perrott, R., Latunde-Dada, K., Oldenbeuving, R.M., Roeloffzen, C.G.H., van Dijk, P.W.L., Hoekman, M., Leeuwis, H., and Leinse, A., "Optical beamforming based on microwave photonic signal processing," Proc. 10562, International Conference on Space Optics — ICSO 2016; 1056221 (2017).

[5] Palffy-Muhoray, P., "Orientationally Ordered Soft Matter: The Diverse World of Liquid Crystals," *electronic-Liquid Crystal Communications*, (2007).

[6] Desimpel, Ch., [Liquid Crystal Devices with In-Plane Director Rotation], PhD thesis, Ghent University (2006).

[7] Bahadur, B, "Liquid Crystal Displays," Molecular crystals and liquid crystals 109 (1), 1-98 (1984).

[8] http://www.phoenixbv.com/index.php

[9] Bobrovsky, A., Ryabchun, A., and Shibaev, V., "Liquid crystal photoalignment by films of side-chain azobenzene-containing polymers with different molecular structure," J. Photochemistry & Photobiology A: Chemistry 218 (1), 137-42 (2011).

[10] Wang, X.Q., Srivastava, A.K., Fan, F., Zheng, Z.G., Shen, D., Chigrinov, V.G., and Kwok, H.S., "Electrically - optically tunable photo-aligned hybrid nematic liquid crystal Dammann grating," Opt. Lett. 41, (24), 5668-71 (2016).

[11] http://www.vescent.com/manuals/doku.php?id=waveguide:manual